A Midlatitude Squall Line with a Trailing Region of Stratiform Rain: Radar and Satellite Observations[1]

BRADLEY F. SMULL AND ROBERT A. HOUZE, JR.

Department of Atmospheric Sciences, University of Washington, Seattle, WA 98195

(Manuscript received 28 March 1984, in final form 4 September 1984)

ABSTRACT

A squall line exhibiting an extensive trailing region of stratiform precipitation passed over the observational network of the National Severe Storms Laboratory on 22 May 1976. Satellite imagery and conventional radar observations document its evolution from a broken line of thunderstorms to a system of mesoscale proportions, and single-Doppler radar observations describe aspects of its mature structure. Satellite measurements of cloud-top temperature showed the system to be a mesoscale convective complex (MCC). The life cycle of the system exhibited the stages of development seen in tropical cloud clusters.

At maturity, two prominent mesoscale flow regimes were identified at midlevels: one marked by inflow into the system's front and continuing toward its rear, and another associated with inflow entering the extreme rear of the system.

The rear inflow was associated with a cyclonic midlevel vortex in the stratiform precipitation region. It produced a concavity, or "notch", in the back edge of the precipitation echo. Shortly after the appearance of the notch, a downwind segment of the leading convective line accelerated forward. The notch persisted through the dissipating stage, at which time secondary notches also formed. The last remnant of the stratiform precipitation area took the form of a chain of three comma-shaped vortices, whose origin could be traced in time back to the primary and secondary notches.

The inflow at the front of the system spanned both the leading convective and trailing stratiform regions. Convective-scale velocity maxima were superimposed on this front-to-rear flow in the convective region, while a broad maximum of the rearward current occurred in the stratiform region, just above the melting layer. This rearward system-relative flow apparently promoted the broad structure of the precipitation area. Slowly falling ice particles originating at convective cell tops were evidently advected rearward and dispersed over a 50–100 km wide region, whereupon their melting produced a prominent radar bright band.

1. Introduction

Middle latitude squall lines possessing extensive regions of trailing light precipitation have been described by Newton (1950), Fujita (1955), and Pedgley (1962).[2] On 22 May 1976, such a system passed eastward over Oklahoma and traversed the observational network of the National Severe Storms Laboratory (NSSL). This network included nine rawinsonde sites and NSSL's conventional and Doppler radars. Ogura and Liou (1980; hereafter referred to as OL) used the NSSL soundings to perform a kinematic and thermodynamic study of the 22 May 1976 squall system. They noted the similarity of this type of midlatitude squall system to tropical squall lines (Zipser, 1969, 1977; Houze, 1977). Detailed, three-dimensional radar reflectivity observations have been useful in studying the life cycles and stratiform regions of tropical cloud systems (Houze, 1977; Leary and Houze, 1979a,b; Houze, 1981; Churchill and Houze, 1984; Houze and Rappaport, 1984). Ogura and Liou recommended that a detailed radar study be undertaken of the 22 May 1976 Oklahoma squall line. In addition to documenting the reflectivity in the trailing stratiform region (especially the melting layer), the radar data collected for this case included Doppler radial velocities, thus allowing the air motion field associated with the reflectivity structures to be examined in much more detail than was permitted by the sounding data analyzed by OL.

A primary objective of this paper is to reveal the radar-echo structure of both the trailing stratiform region and the leading convective line of the 22 May 1976 Oklahoma squall system. The Doppler radar data were obtained while the system was in its mature stage. Hence, it is for this time that we have constructed the most detailed analyses of the storm's internal flow features and corresponding fine points of the radar echo pattern.

To put these analyses into the context of the storm's life cycle, we also report here on the history of the system, from initiation through dissipation. A

[1] Contribution No. 728, Department of Atmospheric Sciences, University of Washington.

[2] Other types of squall lines occur in midlatitudes; for example, the sort described by Newton and Fankhauser (1964). Here we are concerned only with the type characterized by a broad trailing region of light rain.

mesoscale system studied by Pedgley (1962) went through a life cycle in which the storm began as a line of discrete cumulonimbus cells. These cells grew and eventually merged to form a continuous convective line trailed by a region of light rain falling from a widespread altostratus cloud layer, which was connected to the rear of the line. When the convective line dissipated, the system lingered as a slowly decaying region of altostratus and light rain. Pedgley presented a conceptual model of each major stage of development of the system. However, much remains to be understood about how such a system evolves from one stage to the next. Pedgley's study was carried out without benefit of satellite or high quality radar observations. A major objective of our description of the 22 May 1976 Oklahoma squall system is to present satellite and detailed radar views of the life cycle of a system very similar to that described by Pedgley.

Our satellite overview of the life cycle of the 22 May 1976 squall system documents the evolution of its visible cloud structure (prior to sunset) and its cloud-top temperature pattern. Maddox (1980, 1983) has used cloud-top temperature to identify the "mesoscale convective complex (MCC)." Only a little work (e.g., Leary and Rappaport, 1983; Rockwood *et al.*, 1984) has been done as yet to describe the radar echo patterns underlying MCC cloud shields. As we will show, the cloud shield of the 22 May 1976 squall system satisfies the definition of an MCC. We do not suggest that this storm possesses the only type of convective organization that produces an MCC cloud shield. Nonetheless, a major objective of our study is to show the radar echo and details of the airflow within one example of an MCC. It remains for future studies to determine if the pattern we describe is typical or just one of many that can occur.

2. Data and methods of analysis

The principal source of data used in this study was the 1976 NSSL Spring Program network (Fig. 1). On 22 May, soundings were released at the NSSL sites: first at 0900 CST (all times CST hereafter) to assess the potential for later activity, and subsequently over the period 1300–2330 at intervals of about 90 min, documenting the squall line's passage. Surface conditions (basic meteorological parameters including accumulated precipitation) were recorded at NSSL's 14 subsynoptic stations and digitized at one-minute intervals. Sounding and surface data have been examined to aid interpretation of satellite and radar information.

The NSSL's *S*-band (10 cm wavelength) WSR-57 radar at Norman measured the radar reflectivity in full-azimuth scans and tilt sequences, which were documented by scope photography at 20 s intervals. In addition, three *S*-band Doppler radars were deployed (see Fig. 1). No useful velocity data were provided by the CHILL radar; however, data from NSSL's Norman and Cimarron radars were of high quality.

In this paper, we have restricted ourselves to single-Doppler analysis. Dual-Doppler synthesis of the wind

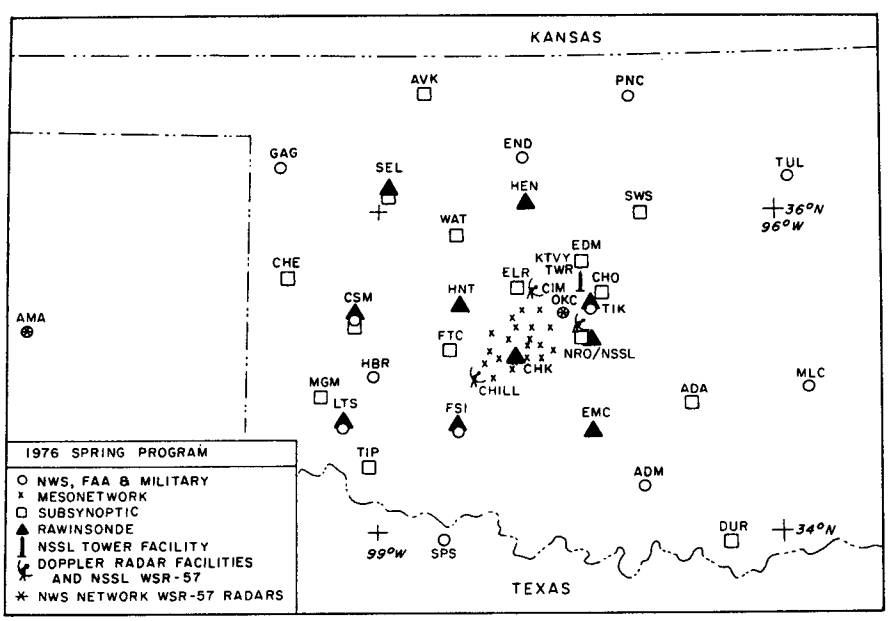

FIG. 1. Deployment of sensors in 1976 NSSL Spring Program (based on NSSL reports). CIM, NRO/NSSL and CHILL denote locations of Doppler radars; for other three-letter station designations see text. Sensor types are indicated in legend.

field from the two NSSL Doppler radars is underway and will be reported in a future paper. However, the results presented here show features of the storm that cannot be seen in the dual-Doppler synthesis. Since they are less restricted in range, the single-Doppler data provide a range–height cross sectional view that extends completely across the system, from the leading pre-line convective anvil to the trailing edge of the stratiform region. The single-Doppler measurements useful to this study are, however, limited to a relatively small portion of the system's total length. Since dual-Doppler synthesis is more restricted in range, it provides no insight into the airflow at the rear of the system. On the other hand, the dual-Doppler area extends over a large portion of the system's total length, and thus provides an assessment of variations in the along-line direction. Because of the different types of information provided by the single- and dual-Doppler studies, we have found it to be most clear to present their results separately.

Doppler measurements were principally limited to that volume occupied by precipitation, and the "internal" aspects of system structure thereby derived are emphasized here. Rawinsonde data, however, allow the identification and extension of mesoscale airflow regimes beyond these limits, and provide valuable thermodynamic data throughout the system and its environment. Only a small portion of these data is referred to in the present study. A thorough analysis of the rawinsonde measurements will be presented later in a study focused on the interrelationship of the flows internal and external to the precipitation area.

Since Cimarron was closest to the echo and best sampled its full extent, its data were chosen for single-Doppler analysis. As the squall system moved into range of the Cimarron radar, data were recorded beginning at 2000 at azimuths primarily between 230° and 280°. Vertical structure was observed by running the radar through a sequence of elevation angles within the azimuth sector scanned. Sampling of a complete volume was typically completed in 5 to 8 min. Volume scans centered at 2042 and 2135 together describe the total front-to-rear extent of the echo near maturity. After 2200, both NSSL Doppler radars were oriented to view the leading convective line only.

Radial velocities were corrected for elevation angle to yield the horizontal velocity component in the radial direction. The contribution of the particle fall velocity component along the beam was neglected. This simplification introduces only small errors. We estimate that errors of up to 1–3 m s^{-1} in the derived horizontal wind speed are possible in a few locations. However, these perturbations (if present) do not affect the results of our study.

Since the system formed beyond the range of the NSSL radars, and because NSSL data collection ended at 2330, scope photography from the National Weather Service's WSR-57 radars at Amarillo and Oklahoma City has been employed to describe the formative and dissipative stages of the system's life cycle, respectively. Satellite data used in this study are the standard visible and enhanced infrared images available at 30 min intervals from the GOES-East satellite.

3. Satellite overview

The organization and evolution of the squall-line system was well documented by visible and enhanced infrared satellite imagery (Fig. 2). Preceding the development of precipitation, a field of altocumulus extended from central New Mexico eastward to the west-central Texas panhandle. Initially these altocumuli were rather benign in appearance, but by 1300 (Fig. 2a) a distinct band of enhancement corresponding to growing convective clouds (including several newly issued anvil clouds) had developed along a north–northwest to south–southeast axis straddling the Texas–New Mexico border. The first radar echoes appeared at the northern end of this band. Deep convection developed rapidly, and by 1400 (Fig. 2b) numerous anvils were visible. A secondary line of convection (denoted CR in Fig. 2b) appeared ahead of the main band. This development occurred near the region's most outstanding topographical feature, the "Cap Rock" escarpment. (The possible influence of this topography on the development of deep convection was noted by Fankhauser, 1971). Also apparent was a separate cluster of cumulonimbus in the northwest Texas panhandle, and another area of developing storms over west Texas in proximity to a branch of the polar jet stream, which extended from northern Mexico into southwest Texas.

At 1600 (Fig. 2c), the developing squall line was quite prominent, appearing as several conglomerates of cumulonimbus aligned and merging in the central Texas panhandle. Anvils emanating from the secondary line of convection had been absorbed by the squall line's expanding cirrus shield and therefore are not explicitly seen in Fig. 2c. Marked changes were apparent in the system's wake, where the extensive field of altocumulus was interrupted by an expanding clear area. Other observations showed that this clearing coincided with a shallow wake of air from convective downdrafts, which appreciably stabilized the post-squall region.

Near the time of sunset (Fig. 2d), the squall system appeared as a solid, oval mass of upper-level cloud centered near Oklahoma's western border. The extent of the cloud shield increased rapidly, its width measuring twice that shown two hours earlier. In contrast to the dominant leading anvil extending eastward from the isolated thunderstorm in west-central Texas, cloud spread more symmetrically about the squall-

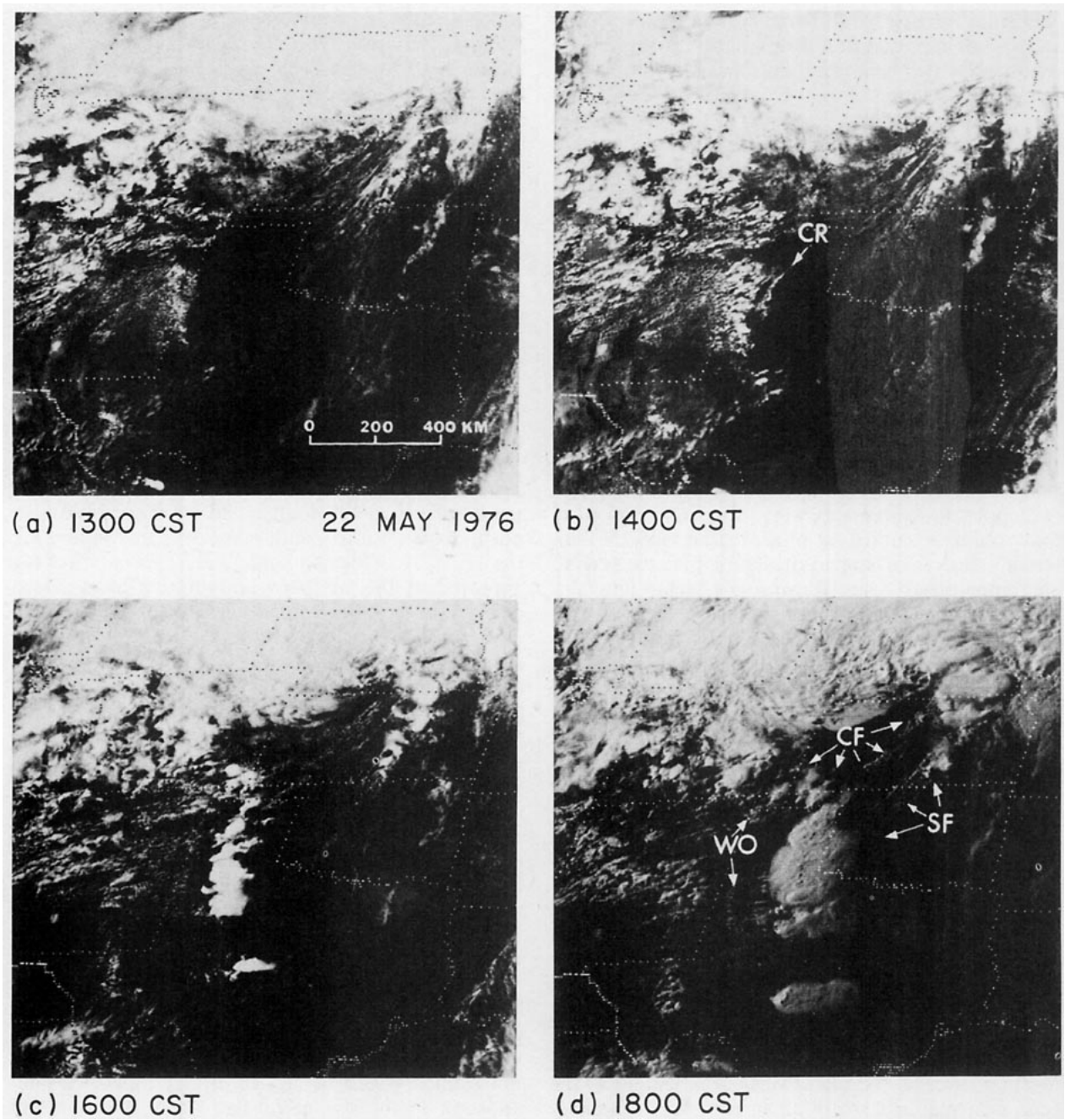

FIG. 2. Sequence of GOES-East visible and enhanced infrared imagery illustrating evolution of squall-line system during 22-23 May 1976. Annotated features are described in text. Due to navigation error, all gridded political/geographic boundaries should be shifted 50 km northwest from their indicated positions. Scale shown in (a) is strictly true at 34°N, 100°W, but accurate to within 5% over the region of interest. Temperature thresholds for enhanced infrared images are −32.2 (medium gray), −42.2 (light gray), −53.2 (dark gray), −59.2 (black), −63.2 (black to white), and −71.2°C (white).

line thunderstorms, which were visible as a north–south line of small shadows cast by cumulonimbus towers penetrating above the equilibrium level. These cloud tops were associated with the developing radar echo line, to be described. Especially significant is that the rear cloud edge trailed the line of convective cells by more than 100 km—much beyond the distance typically spanned by "back-sheared" anvil clouds observed in association with thunderstorms occurring in more strongly sheared environments (e.g., the storm in west-central Texas; also see the schematic visual appearance of a supercell thunderstorm depicted in Fig. 16 of Houze and Hobbs, 1982). Ahead of the squall system, a line of towering cumulus

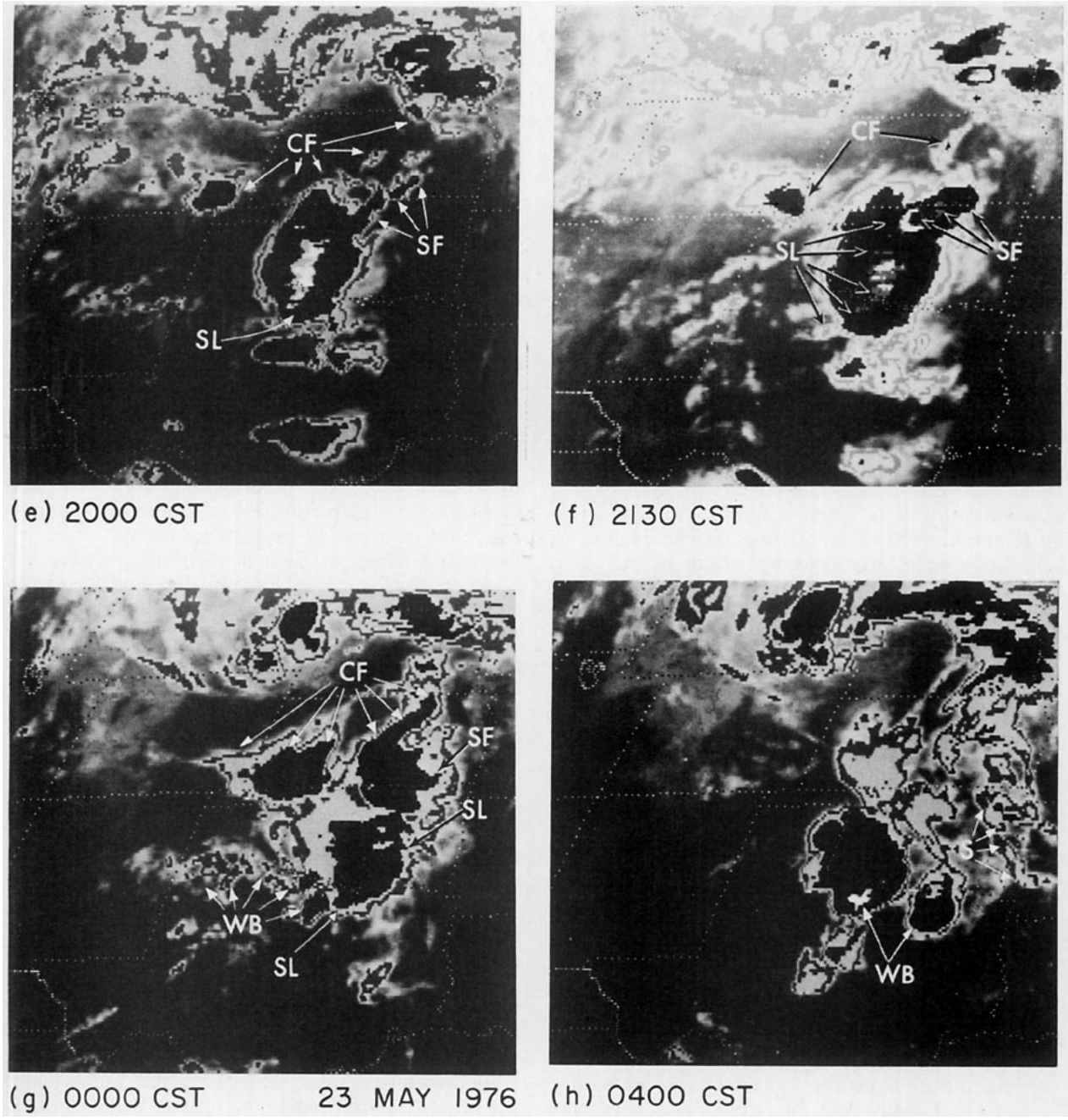

FIG. 2. (*Continued*)

(destined to interact with the squall line and denoted SF in Fig. 2d) was associated with a weakening stationary frontal zone and extended from south-central Kansas southwestward toward the northern end of the squall line. Another band of developing convective clouds (CF) accompanied a surface cold front advancing southeastward over western Kansas. To the squall system's rear, an arc of cloudiness (WO) marked the extent of the expanding wake of outflow air. Scattered nonprecipitating clouds that developed rapidly within the wake (i.e., between WO and the back of the squall line anvil) probably resulted from the upslope character of easterly winds observed there.

The cold cloud shield seen in Fig. 2e satisfied the definition of a "mesoscale convective complex" (MCC) according to Maddox (1980); the area of temperatures below −52°C exceeded 50 000 km^2 from about 1800 22 May to 0030 23 May. Its area was 90 000 km^2 at the time of Fig. 2e. At this time,

the convective cells were near their peak intensity, appearing as a north–south line of light grays (SL), corresponding to cloud-top temperatures $< -63°C$. A segment of cold cloud (SF) jutting northeastward from the oval cloud shield marked convective cells developing along the weak stationary front. To the north, convection continued in a broken fashion along and just behind the surface cold front (CF).

The mature system is shown in Fig. 2f, during the period that Doppler radar data collection was underway. The cloud's dimensions (i.e., that area of temperatures $< -32°C$) had increased to a maximum width of 450 km and length of 500 km; its total area was in excess of 170 000 km^2, with the region enclosed by the $-52°C$ contour measuring over 130 000 km^2. While still apparent, the area of extremely cold cloud associated with squall-line convection had decreased. The line of coldest, highest cloud tops (SL) took on an elongated "S" shape. The aforementioned pre-squall convection associated with SF again jutted outward at the cloud shield's northeast corner.

At about 0000 (Fig. 2g), the system entered its dissipating stage. Although the extent of the cloud shield trailing the squall line continued to increase, with a broad region of relatively uniform temperatures found toward the system's rear, the upper-level cloud shield had lost its highly organized structure. Contours of cloud-top temperature no longer formed an elliptical pattern centered on the squall-line convection, but had degenerated into several local minima. The southeasternmost of these (denoted SL) marked the remaining arc of squall-line convection, which advanced rapidly southeastward while weakening. A broken line of cold clouds just south of the squall system's track (denoted WB) was associated with thunderstorms forming and intensifying along a boundary constituted by the wake outflow. The situation along the wake's northern edge was complicated by the influence of the weak cold front (CF). A surge of cool northwesterly surface winds accompanying the front interacted with the wake in a manner unresolved by available observations, but both influences were likely important in sustaining the strong convection seen along the Kansas–Oklahoma border.

By 0400 23 May (Fig. 2h), clouds associated with active convection along the squall system's leading edge had disappeared. The once extensive upper-level cloud shield had largely dissipated, as indicated by higher temperatures and a thinner appearance of clouds over much of the eastern two-thirds of Oklahoma. Several elongated patches of colder cloud remained, oriented from northwest to southeast. The cloud bands over extreme eastern Oklahoma (collectively denoted S) coincided with the last traces of stratiform precipitation associated with the squall system, while the patch over the north-central part of the state corresponded to a small area of weak convective cells that developed within the trailing wake region. (These features are described further in Section 4). Also evident at this time were the rapidly expanding upper-level cloud shields associated with thunderstorms intensifying along the wake's southern edge. Although these storms moved east–southeastward, their cold anvils spread northeastward to cover much of southwest Oklahoma.

4. Evolution of the radar echo pattern

The organization and development of precipitation falling from the cloud structures illustrated in Fig. 2 are shown by plan views of reflectivity from the Amarillo, Norman and Oklahoma City WSR-57 radars (Figs. 3–5). (The locations of these radars are denoted as AMA, NRO/NSSL and OKC, respectively, in Fig. 1.) The squall system originated at about 1230 as a group of isolated showers (Fig. 3a) falling from the developing cumulonimbus clouds seen west of the Texas–New Mexico border in Fig. 2a. This period, in which the system consisted of a group of separate cells, was referred to as the "formative" stage by Leary and Houze (1979a) in their study of the life cycle of tropical mesoscale systems. The formative stage continued for several hours; in the interval 1300–1400, radar echoes developed north of and even more extensively south of the initial cluster of cells, forming a band 300 km in length oriented from north-northwest to south-southeast (Fig. 3b). The cells northwest of the radar moved less rapidly than those aligned to the southwest, and apparently were not part of the organized system. A secondary line of convective cells, associated with cloud feature CR in Fig. 2b, developed rapidly and is similarly labeled in Fig. 3c. These echoes remained nearly stationary along the Cap Rock escarpment, and hence were rapidly overtaken by the developing squall line.

During a 4–5 h period following the appearance of the first radar returns, the echo pattern remained a collection of discrete cells. However, during this time the upper-level anvils of the individual cumulonimbus were merging (Fig. 2c). By 1800 (Figs. 2d and 3d), when the merger was complete and had formed a single widespread anvil, lighter precipitation was filling the spaces between individual cells so that the squall system comprised one large, continuous radar echo. This period of development was referred to by Leary and Houze (1979a) as the "intensifying" stage. In this case, the intensifying stage lasted only about one hour. By 1900 (Fig. 3e), the echo's rear edge had taken on a more diffuse appearance, marking weak horizontal reflectivity gradients indicating that stratiform precipitation was spreading to the rear of the convective line. This development marks the beginning of the "mature" stage in the Leary–Houze terminology. Recalling again that the first cells were seen at 1230, we note that about 6.5 h passed before a stratiform echo first became apparent on radar.

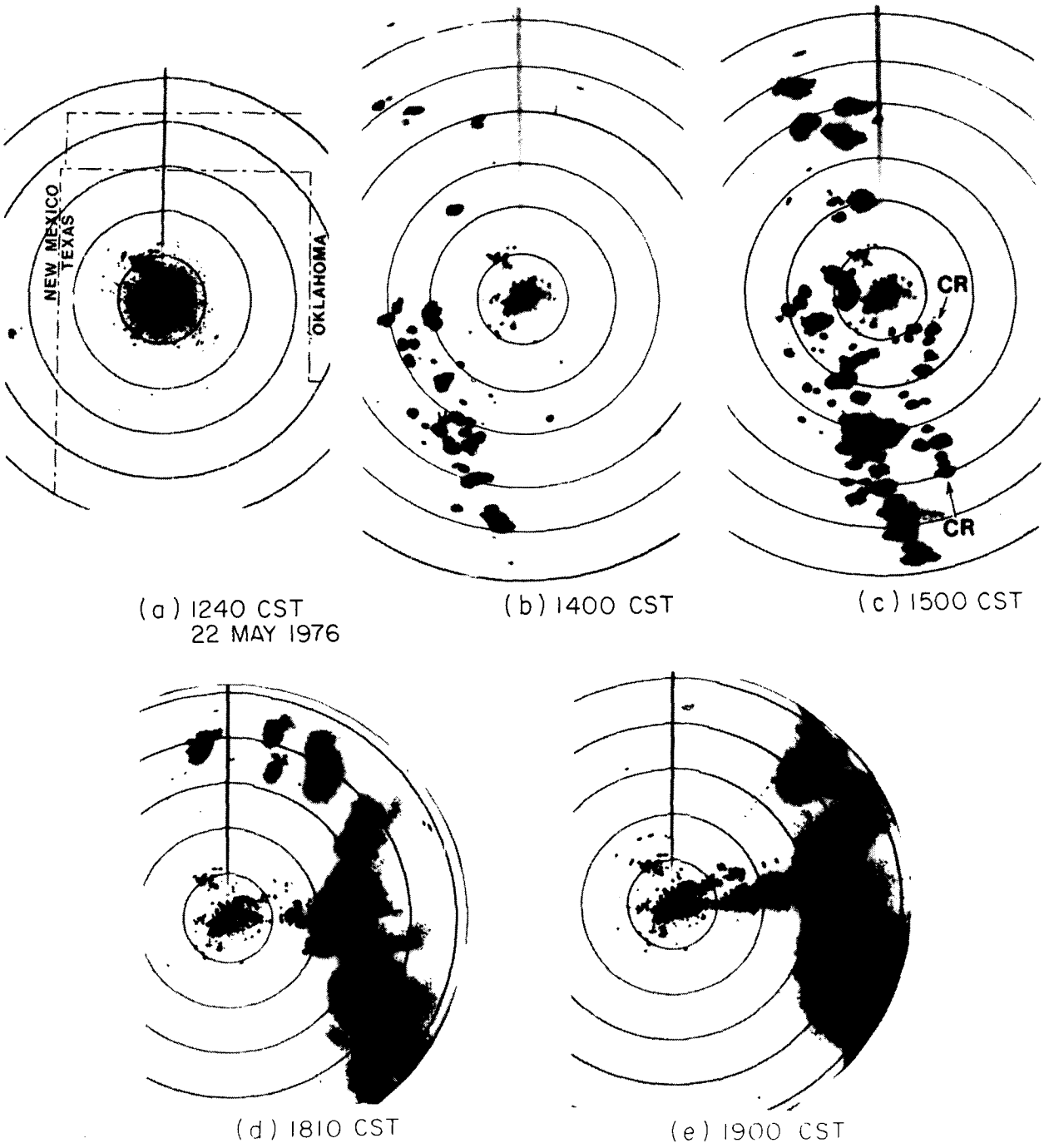

FIG. 3. Low-elevation PPI displays of nonintegrated video from Amarillo (AMA) WSR-57 radar showing formation and development of squall line on 22 May 1976. Range circles are at 46 km intervals. In (c), CR denotes a secondary line of cells (see text).

This time scale of development is consistent with that found in tropical mesoscale systems, for which observations showing the time variation of convective and stratiform precipitation amounts indicate that typically 4–8 h passes between initial convective cell formation and the appearance of stratiform precipitation adjacent to the cells (Houze, 1977; Leary, 1984; Churchill and Houze, 1984; Houze and Rappaport, 1984).

An extensive area of false echoes developed between the radar and the rear of the precipitation echo at about the time that the stratiform rain appeared. These echoes evidently resulted from the refraction of the beam toward the earth's surface by a strong

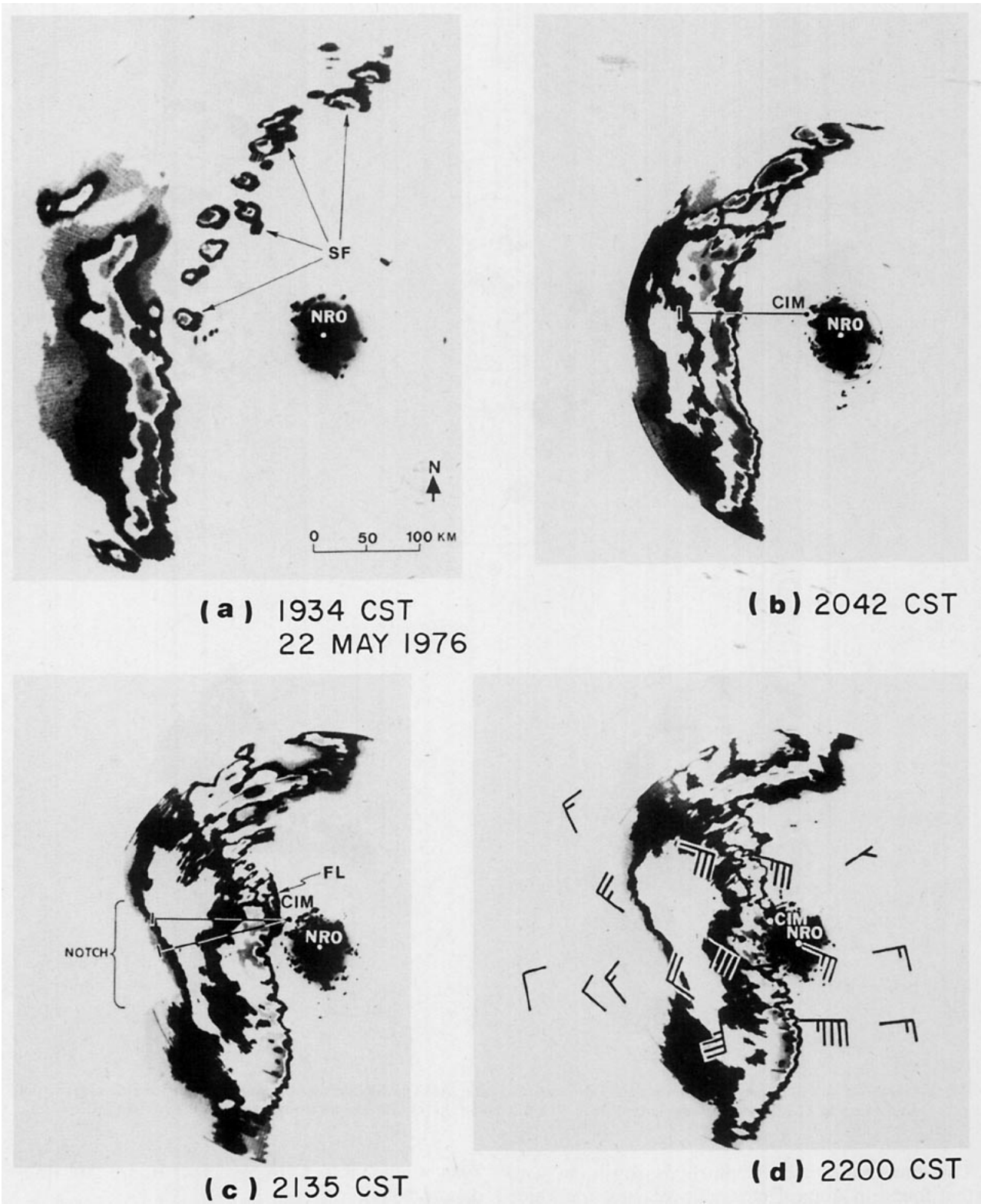

FIG. 4. 0.8° elevation PPI displays showing horizontal reflectivity structure of mature squall-line system over Oklahoma. Data are from the WSR-57 radar at Norman (NRO). Azimuth lines from the Cimarron Doppler radar (CIM), along which vertical cross sections in Figs. 7–9 were taken, are indicated in (b) and (c). In (a), SF denotes pre-squall cells along weak stationary front; in (c), FL indicates fine-line echo. Azimuths drawn from CIM are 270° in (b), and 270° (northern line) and 255° (southern line) in (c). Levels of shading denote minimum detectable, 21, 31, 42 and 52 dBZ. The "notch" in (c) is explained in text. System-relative winds at the 600 mb level observed over a 3 h period centered at 2200 are shown in (d). The wind plotting convention is: full barb, 5 m s^{-1}; half-barb, 2.5 m s^{-1}.

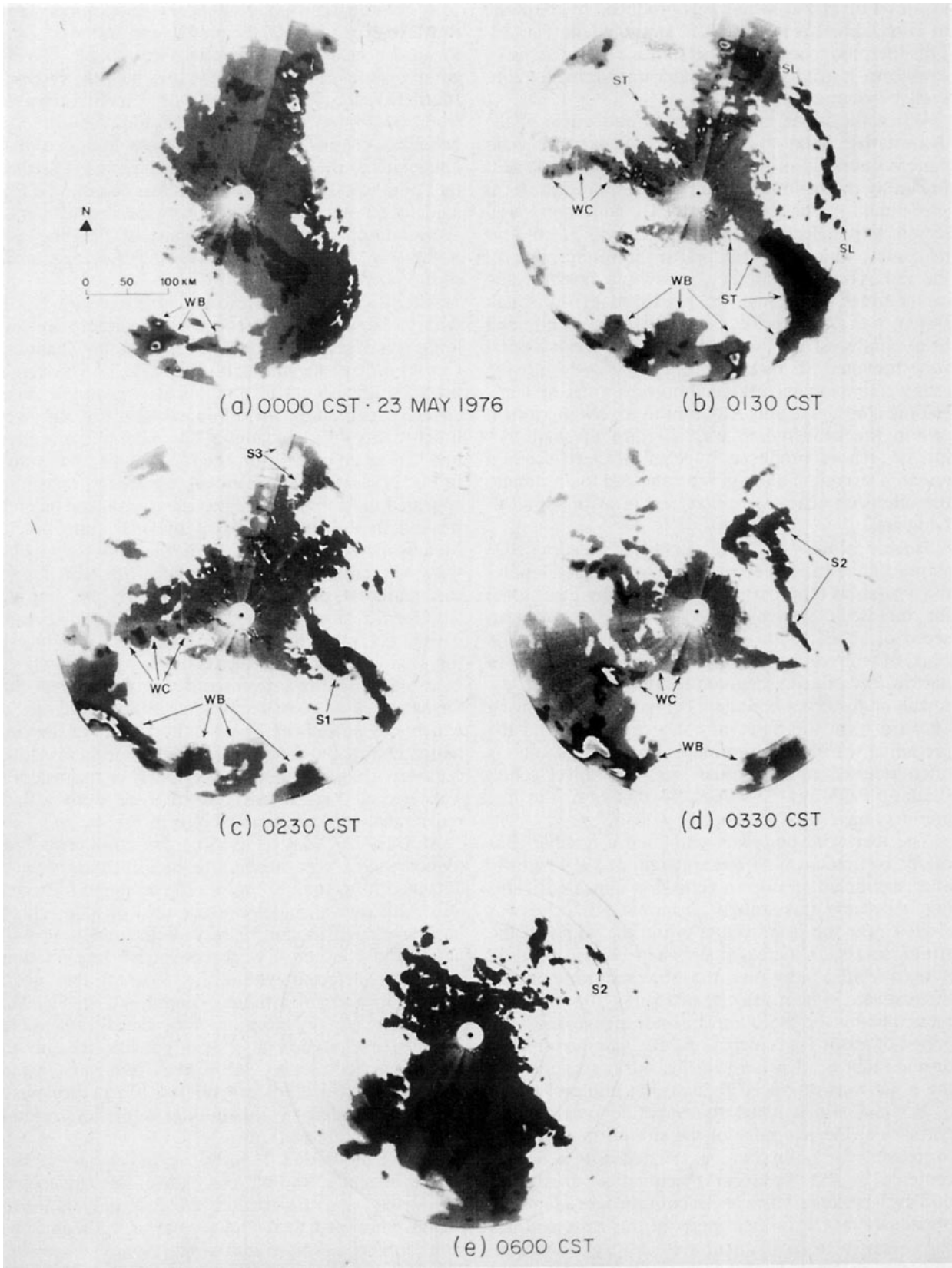

FIG 5. Low-elevation PPI displays of reflectivity from Oklahoma City (OKC) WSR-57 radar showing dissipation of squall system and concurrent development of echoes along and within its wake. Levels of shading (dimly visible in photographs) correspond approximately to minimum detectable, 30, 41, 46 and 51 dBZ. Labeling denotes features discussed in text.

low-level inversion, which was produced by the wake of cool convective downdraft air noted in Fig. 2d. This thermodynamic stratification is characteristic of stratiform rain areas associated with mesoscale convective systems.

When the squall system moved into range of the quantitative radar at Norman (Fig. 4a), the echo pattern consisted of a leading line of convective cells trailed by the region of rapidly developing stratiform precipitation. The latter occupied a wide horizontal region with reflectivity values exceeding 31 dBZ at its center, which is attributed to the interception of the radar bright band at the melting level by the rather broad (2°) radar beam. Ahead of the squall system was a broken line of convective cells oriented from southwest to northeast along the weak frontal zone (denoted SF in Fig. 2e). These slowly moving cells were rapidly incorporated into the squall system's leading convective line. Adjacent to the southernmost cell in the broken line was a group of small but intense echoes produced by chaff released from a research aircraft. The chaff was intended to illuminate the otherwise echo-free inflow region of this intensifying cell.

Isochrone analysis of the squall line's leading edge shows that during the period of our single-Doppler radar analysis (approximately spanned by Figs. 4b–c) the mesoscale system moved eastward at a mean speed of about 15 m s^{-1}. Just ahead of the leading edge of convective precipitation in Fig. 4c lay a narrow line of echo (denoted FL) associated with the squall- or gust-front boundary between cool air flowing outward from the bases of convective cells and the preceding warmer environment. This type of echo is often referred to as a "fine line" or "angel echo" (Battan, 1973, pp. 258–262). In this case, the fine line may have been enhanced by chaff.

The rear echo boundary exhibited a notable concavity, or notch, which was apparent at 1934 (shortly after significant stratiform echo first appeared). This notch became increasingly prominent as echo was eroded near the line's center while the width of the stratiform region increased elsewhere (Figs. 4c and d). System-relative flow (i.e., the observed wind minus the eastward system velocity of 15 m s^{-1}) at 600 mb, measured by the NSSL rawinsonde network over a period of about 3 h centered on 2200, is superimposed on the radar echo pattern in Fig. 4d. It suggests that the notch was produced by a strong midlevel influx of dry air, which acted to evaporate precipitation particles at the rear edge of the stratiform rain area. Moreover, this influx was associated with a vortex centered in the stratiform precipitation area. This midlevel cyclonic vorticity maximum was identified previously by OL in their study of this case, and has been seen in tropical squall systems (e.g., Gamache and Houze, 1982). The evolution of the notch seemed closely related to changes in the shape and motion of the leading convective line; the development and forward expansion of the notch was followed by a forward acceleration and intensification of a downwind segment of the convective line, near the system's southern end. That segment's movement increased from 10–15 to 20–25 m s^{-1} (cf. Figs. 4b–d). This behavior of the leading convective line is rather analogous to the "bow echo" phenomenon described by Fujita (1981); in our case, the rear echo notch was evidently a precursor to the downwind line segment's acceleration. The bowing forward of the line was noted (Fig. 4b) about one hour after the appearance of the notch.

After 2330, no data were available from the NSSL radars. However, the reflectivity structure at low levels was observed by the WSR-57 radar at Oklahoma City (Fig. 5). At midnight (Fig. 5a), the system's precipitation echo had attained its maximum areal coverage, exhibiting a width in excess of 150 km over much of its 400 km length. The leading convective line had taken on an elongated "S" shape (also noted in Fig. 2f) as its southern end accelerated. Convection appeared most intense and persistent along the bulging portion of the line, ahead of the rear echo notch. Meanwhile, other segments of the convective line were weakening (e.g., note the echo-free gaps found east-southeast of the radar), although the trailing stratiform region remained cohesive and widespread. The initial weakening of the convective line marks the beginning of the "dissipating" stage, which in Leary and Houze's terminology occurs when the formation of new convective cells diminishes, but in which the stratiform cloud can persist for several hours. During the dissipating period, strong convective cells were triggered along the periphery of the system's wake (recall Fig. 2g). A few of these were within radar range and are denoted WB in Fig. 5a.

At 0130 23 May (Fig. 5b), the convective line (denoted SL) was weakening rapidly and became detached from the trailing stratiform region (denoted ST). Although an indeterminate area of false echoes had developed in the vicinity of the radar, several bands and clusters of weak convective precipitation cells were detected within the wake of the squall system, in particular those denoted WC in Fig. 5b. The history and organization of the clouds responsible for this precipitation and their possible relation to clouds seen developing within the wake early in the system's life (Fig. 2d) are unclear since they were quickly shrouded by the trailing upper-level cloud shield in satellite pictures.

During the period 0130 to 0230 (Figs. 5c–d), the squall system's leading convective line dissipated completely, and the areal coverage of the stratiform region continued to dwindle. East of the radar, the stratiform echo evolved into several elongated comma-like features (denoted S1, S2 and S3) that moved northeastward. By forming a composite echo pattern

based on the sequence of patterns on the Oklahoma City scope between 0230 and 0310, we have found that S1, S2 and S3 were connected along a line extending north-northwest to south-southeast (Fig. 6). This chain of commas constituted the remaining stratiform precipitation. It lay largely beneath the clouds identified as S in Fig. 2h. Tracing of the echoes in time suggests cyclonic rotation about the comma heads. It thus appears that during the late-dissipating stage of the system, the relative-flow vortex characterizing the stratiform region (Fig. 4d) broke down into several subvortices. The concave rear echo boundary south of the head of S2 could be traced to the primary notch seen earlier. The concave portions of S1 and S3 could also be traced (albeit with some subjectivity) back to secondary notches that appeared north and south of the main notch at about 0000 (Fig. 5a). Bands of weak convective cells west of the radar moved southeastward, in contrast to the northeastward movement of the comma-shaped features. Wind profiles in the wake region show substantial backing through the low to midtroposphere, i.e., a weak northerly component at low levels overlain by a stronger southerly component above. With respect to the observed echo motions, this suggests that the convective cells within the wake were relatively shallow, low-level phenomena, while the stratiform precipitation evidently fell from clouds moving with the mid- to upper-tropospheric flow.

At about 0600 (Fig. 5e), the last bit of stratiform echo traced back to the squall system (S2) was dissipating in northeastern Oklahoma, although an extensive area of precipitation associated with convection initiated along the system's wake continued over central and southern Oklahoma.

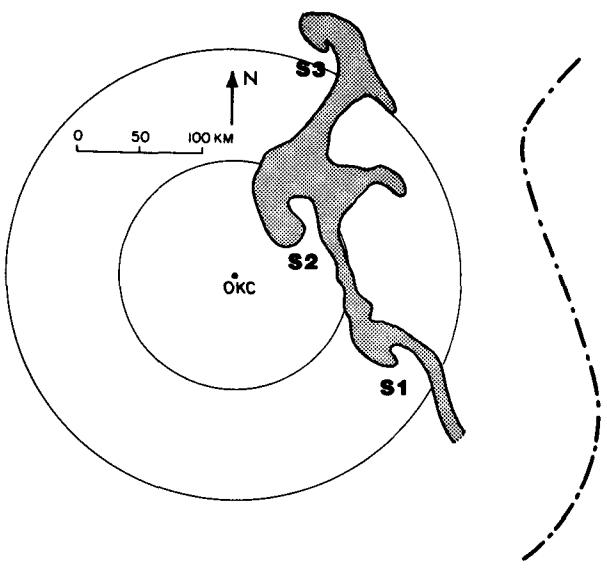

FIG. 6. Composite echo pattern based on Oklahoma City (OKC) WSR-57 radar data for the period 0230–0310 on 23 May 1976. Shading denotes stratiform precipitation echo, which at this time took the form of a chain of comma-like features (S1, S2 and S3). Range circles centered on OKC are at intervals of approximately 93 km. Estimated position of dissipating gust front is indicated by dash-dot line.

5. Air motions and vertical echo structure in the leading portion of the mature system

The leading portion of the mature squall system is illustrated in Fig. 7 by a vertical cross section from the Cimarron Doppler radar, taken along the line shown in Fig. 4b. This and all other cross sections extend to a distance of 114 km, the maximum unambiguous range of the Cimarron radar in 1976. Analyses of reflectivity and the horizontal velocity component in the plane of the section (i.e., normal to the squall line) are presented in Figs. 7a and 7b, respectively.

The cross section of radar reflectivity shows an echo-free layer separating the lower boundary of a leading anvil structure from a low-level clear-air echo. The intense clear-air echo reaching the surface at 50 km is thought to have resulted from the deformation of a curtain of chaff by updraft inflow approaching and beginning to rise over outflow from convective downdrafts. The velocity analysis in Fig. 7b shows the surface gust front (marked by an intense velocity gradient at the downdraft outflow's leading edge) near 56 km.

The main convective cell is identified by a core of high reflectivity near 80 km range in Fig. 7a. An adjacent weak-echo region at between 70 and 75 km identifies the probable location of an updraft supporting this mature convective cell, while a corresponding downdraft was likely coupled with the heavy precipitation core at 80 km. Just above the weak-echo region (or updraft) of the mature cell, a plume of high reflectivity (discussed below) extended horizontally into the leading anvil.

At about 65 km, just ahead of the weak-echo region of the mature cell, a new cell was beginning to appear at a height of 5–6 km, apparently in response to an updraft initiated by low-level convergence along the advancing gust front. Behind the mature cell, at about 95 km, was a broad reflectivity feature exceeding 35 dBZ that apparently marked the collapse of a dissipating convective cell (likely dominated by downdraft) into a stratiform mode. This sequence, consisting of a new cell, followed by a mature cell and subsequently a dissipating cell, lends the system a component of discrete propagation similar to that reported by Browning *et al.* (1976) and Houze (1977). The marked decrease of reflectivity in the lowest two kilometers near 110 km was the forward edge of a transition zone separating the leading convective and trailing stratiform regions.

The horizontal wind component measured by Doppler radar (Fig. 7b) is viewed in a coordinate

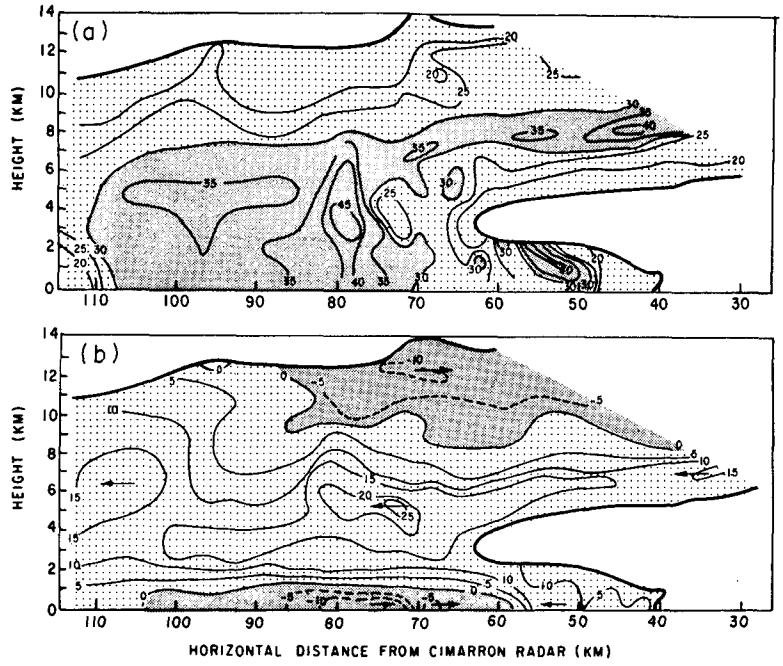

FIG. 7. Vertical cross section through leading portion of squall system (along line in Fig. 4b) at 2042. Fields displayed are (a) reflectivity (dBZ), and (b) horizontal wind component (m s^{-1}) in plane of the section relative to the system. System motion is from left to right at 15 m s^{-1}.

system moving with the squall line, i.e., from left to right at 15 m s^{-1}. The speed of the line exceeded that of its individual cells, since the line's total motion was a combination of continuous cell translation and discrete propagation. The cells in the part of the line shown in the cross section moved with an eastward component of about 6 m s^{-1}; thus, cell-relative velocities may be deduced by subtracting 9 m s^{-1} from the displayed system-relative values, while ground-relative airflow may be obtained by subtracting 15 m s^{-1}.

The system-relative velocity pattern shows strong outflow (negative values) in the lowest kilometer penetrating forward from the convective region toward the clear-air echo, where it strongly converged with low-level inflow toward the squall line. This outflow emanated from the mature and dissipating cells located at 80 and 95 km, probably in association with their combined downdrafts. The maximum outflow speed was located directly below the mature cell.

Above the outflow seen at low levels in Fig. 7b was a layer of positive velocity values between 2 and 8 km, denoting air which flowed into the system's front and continued toward its rear. A prominent maximum of this positive-component flow occurred at the 5–6 km level. An apparently similar feature was identified in rawinsonde data by Sanders and Emanuel (1977). However, the detail afforded by Doppler radar analysis in the case at hand is considerably greater.

Negative velocity components were measured in the upper troposphere above and ahead of the mature cell at 80 km, a result of divergence at the tops of convective updrafts. The dividing point in the flow direction at the top of updrafts in the convective region is consistent with upper-level divergence centered on the squall-line system, a feature characteristic of mesoscale convective complexes (Fritsch and Maddox, 1981; Maddox, 1983). Upper-level detrainment from the cells not only diverted ice particles forward into the leading anvil, but also toward the system's rear, where they entered a regime dominated by stratiform precipitation processes.

Rawinsonde data (analyzed by OL) show that the flow in the large-scale environment ahead of the system was directed toward the squall line at upper levels in the system-relative reference frame. Thus, advection by the environmental wind cannot account for the leading anvil. Its presence must be attributed to the dynamics of convective cells. In the field of cell-relative velocity (obtained by subtracting 9 m s^{-1} from the system-relative flow), the corresponding layer of upper-level forward outflow (negative velocity values) occupied a somewhat deeper region of the anvil—approximately that area above the +10 m s^{-1} contour in Fig. 7b. This flow was evidently responsible for carrying hydrometeors ahead of the line from the tops of cells. The plume of high reflectivity extending forward from the upper portion of the mature cell (Fig. 7a) lay within this layer of cell-relative rear-to-

front flow. The plume no doubt arose as a result of some combination of kinematic and microphysical processes (e.g., horizontal advection, accumulation associated with vertical flux-convergence, evaporation). However, the sequence of events leading to its presence remain unclear. In time, hydrometeors in the plume were transferred by their terminal fallspeeds into the midlevel region of strong inflow. As the particles fell toward the base of the leading anvil, they either completely evaporated or were swept back into the convective region, where they possibly underwent another cycle of growth or played a role in the natural "seeding" of convective updrafts (Carbone, 1982; Rutledge and Hobbs, 1983).

The Doppler velocity cross sections, as well as rawinsonde data shown in Fig. 4d, indicate a mesoscale region of relative movement of air toward the rear of the squall line at middle levels. However, superposed on this broad flow were perturbations resolved only by the detailed Doppler measurements. These took the form of maxima of front-to-rear flow on the order of 10 km in horizontal scale, such as that seen extending rearward from the weak echo region of the mature cell in Fig. 7. These small-scale maxima suggest that convective cell dynamics contributed significantly to (or possibly drove) the broader front-to-rear relative flow spanning the system at midlevels.

6. Air motions and vertical echo structure in the trailing portion of the mature system

Vertical cross sections taken along the lines indicated in Fig. 4c are shown in Figs. 8 and 9. At the time these data were obtained, the squall line was too close to the Cimarron radar for the leading anvil and low-level clear-air echoes to be observed. However, the remainder of the precipitating system was almost completely within the radar's unambiguous range.

The reflectivity pattern in Fig. 8a again exhibits cell structure consistent with discrete propagation. At a range of 15 km, an incipient cell was detected aloft (above a height of 3 km). This cell was followed by a weak echo region at 18 km range, adjacent to a mature precipitation cell between 20 and 26 km. A weaker, dissipating cell was found between 31 and 38 km. The reflectivity pattern indicates that the convective cells were appreciably sloped, suggesting that the embedded convective drafts took on a slope toward the rear of the system with height as well. Major features of the velocity pattern (Fig. 8b) are similar to those described in the context of Fig. 7b. The mature-cell updraft apparently diverged to feed forward- and rearward-directed flows at anvil level, while its downdraft was deflected so as to rush forward toward the leading gust front. The strongly tilted dissipating cell also evidently sent downdraft air forward toward the gust front. (Although a thin surface layer of downdraft air directed rearward into the trailing wake region was indicated by rawinsonde and surface network data, its vertical scale and location precluded detection by Doppler radar.)

The extensive region of light precipitation to the rear of the cells exhibited a pronounced bright band just below the melting level, indicated by a layer of maximum reflectivity between 2 and 4 km in height and extending from 40 to 114 km range, or over a distance of more than 70 km. This melting band stretching across the trailing region is strikingly similar to that found in tropical squall systems (Houze and Betts, 1981), and indicates that stratiform precipitation processes dominated the trailing portion of the system. Separating the convective and stratiform regimes at low levels was a reflectivity minimum, which was referred to in Section 5 as the transition zone.

The system-relative velocity field (Fig. 8b) shows a branch of rear-to-front flow exiting the trailing stratiform region, which was apparently reinforced by downdrafts issued by convective cells forward of 45 km. Elsewhere, velocities were positive (toward the rear of the system); the midlevel maximum rearward flow lay just above the melting band. Atlas *et al.* (1963) and Houze (1981) have shown that a melting band on the order of 100 km in horizontal extent can be explained by the relative horizontal motions of ice particles falling from the upper reaches of a continually regenerating region of convection. The relative flow indicated in Fig. 8 advected ice particles rearward from the tops of the mature and dissipating convective cells. The results of two-dimensional ice-particle trajectory calculations (similar to those of Atlas *et al.*, 1963, and Houze, 1981) are shown in Fig. 8c. For particles originating at heights between 9 and 10 km at the rear of the convective region, fallspeeds between 1 and 4 m s^{-1} result in trajectories that pass through the 0°C isotherm level (near 4 km) over the region spanned by the melting band.

The reflectivity pattern in Fig. 9a is similar in its major features to that shown in Fig. 8a. A difference arises, however, from the fact that the line along which Fig. 9 was taken reached the notch at the back edge of the trailing echo, whereas the line along which Fig. 8 was taken did not (note cross-section projections in Fig. 4c). Thus, Fig. 9b shows the horizontal wind component near the center of the notch. In contrast to the positive velocities found elsewhere in the trailing region at middle levels, negative components were measured along the concave perimeter of the notch. These Doppler radar measurements thus confirm that the notch marked a region of midlevel rear inflow, as indicated by the rawinsonde measurements presented in Fig. 4d. The reversal of the direction of horizontal flow in the vicinity of the notch is also consistent with the midlevel convergence that OL found to be present in the trailing anvil region. During the Doppler analysis

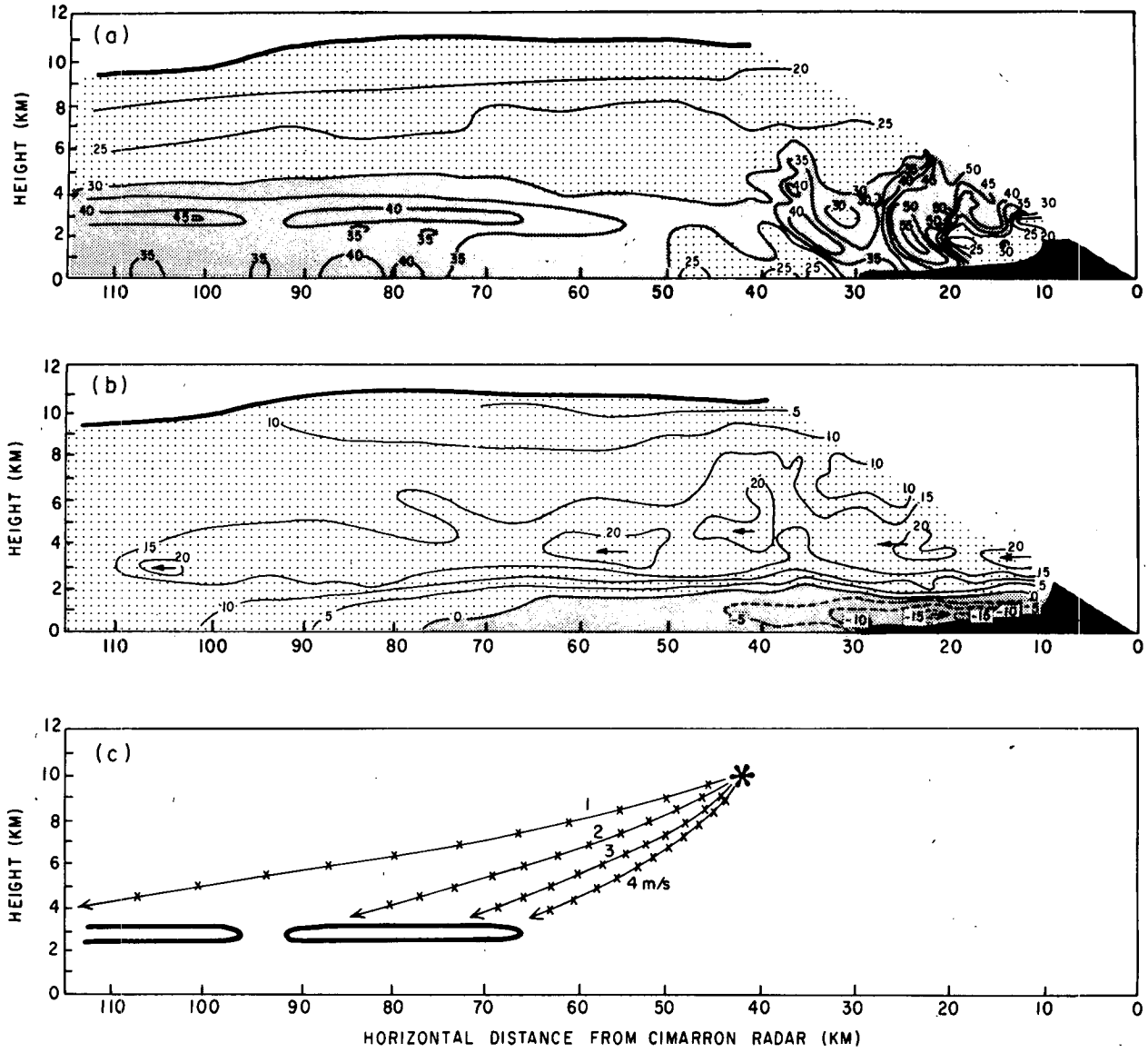

FIG. 8. As in Fig. 7, except for the trailing portion of the system at 2135 (along the northern line in Fig. 4c). Dark stippling inside 30 km range marks the extent of ground clutter and range-folded echo. In addition, (c) displays two-dimensional ice particle trajectories deduced using the Doppler observed horizontal wind component [from (b)] and a range of assumed particle fallspeeds (labeled 1–4 m s^{-1}). Also shown in (c) is the 40 dBZ contour marking the bright band.

period, this flow reversal was limited to midlevels in the vicinity of the notch, although rawinsonde data indicate that the rear inflow later descended and advanced toward the leading convective line, evidently causing it to rapidly bow forward. The erosion of echo illustrated by the 25 dBZ contour near 110 km in Fig. 9a is consistent with the evaporation of falling precipitation particles within the midlevel airstream entering the system's rear.

7. Conclusions

Satellite and radar observations have revealed details of the structure and life cycle of a midlatitude squall line possessing an extensive trailing region of stratiform precipitation. The satellite data show that the system was a mesoscale convective complex (Maddox, 1980), while the radar data illustrate that the stages in its life cycle corresponded to those identified by Leary and Houze (1979a) for analogous cloud systems in the tropics.

The system began as a band of rainshowers falling from discrete cumulonimbus clouds. At about 6.5 h into the system's development, stratiform precipitation appeared behind the convective line and the system entered a period of rapid growth and intensification. The time required to reach this stage of development

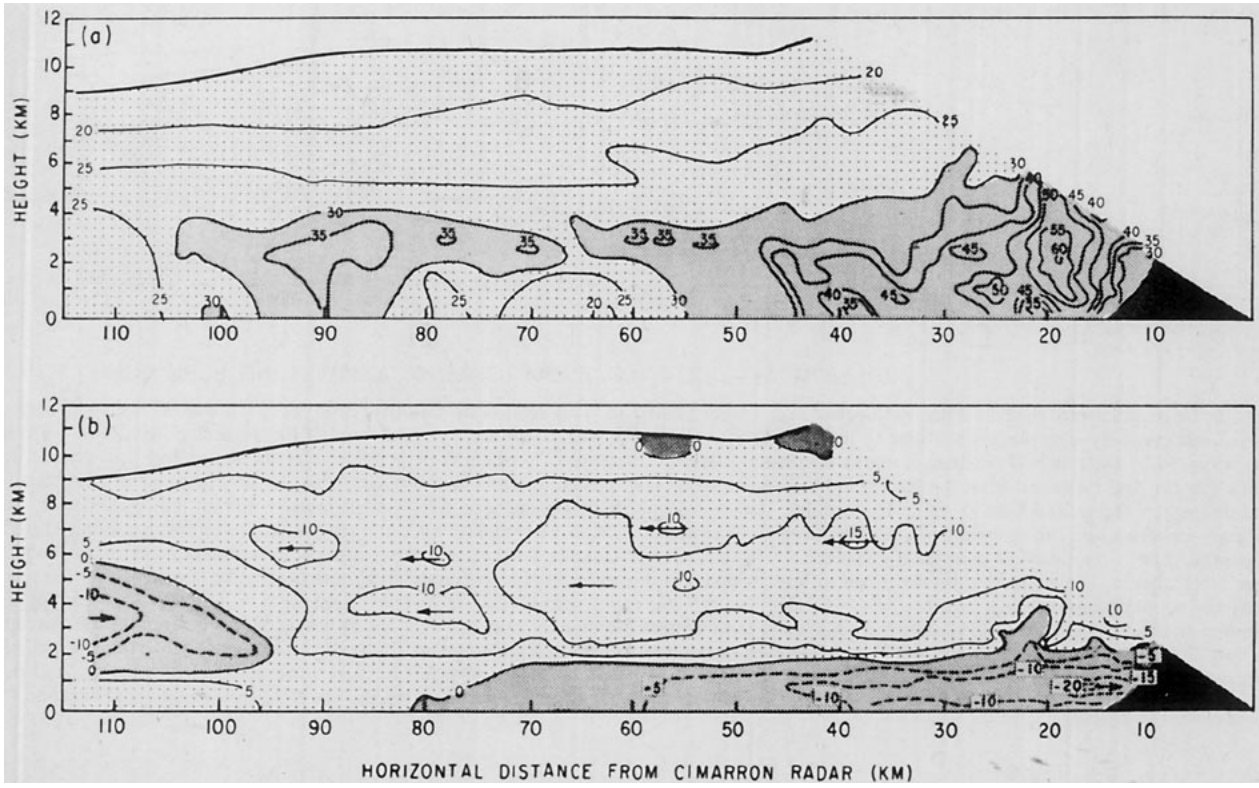

FIG. 9. As in Fig. 7, but extending over the trailing portion of the system toward the center of the rear echo notch at 2135 (along the southern line in Fig. 4c). Component of system motion in plane of section is from left to right at approximately 14.5 m s^{-1}. Dark stippling inside 30 km range, marks the extent of ground clutter.

was quite similar to that observed in tropical mesoscale convective systems. The stratiform precipitation area exhibited a concavity, or notch, on its central rear edge. The notch coincided with an influx of dry air associated with a midlevel cyclonic vortex (in the relative flow) in the stratiform rain area. The notch was apparently related to a subsequent bowing forward of a downwind segment of the leading convective line. The stratiform precipitation area (and the total system rain area) reached maximum size at midnight, some 12 h after system initiation. During the system's dissipating stage, the notch penetrated more deeply into the stratiform region, and the leading convective line continued to accelerate forward, resulting in its separation from the stratiform echo. All but the apex of the contorted convective line dissipated soon thereafter, and those few cells surviving rapidly moved away from the stratiform cloud and precipitation. The latter, however, persisted for another 6 h, until about 18 h after system initiation. By 15 h after initiation, the stratiform rain area had evolved into a north-northwest to south-southeast line of tenuous echo, which was distorted into a chain of comma-shaped features. These commas suggest that the midlevel vortex in the mature stratiform region broke down into a series of subvortices.

The Doppler radar data were taken during the mature stage of the system, while the stratiform area was well developed and growing, the notch was prominent, and the acceleration of the southern portion of the intense convective line was occurring. The Doppler data confirm that the notch was a region of rear inflow and reveal a variety of details of the squall system's internal structure. These are summarized schematically in Fig. 10. The schematic is idealized in that not every section constructed from the single-Doppler measurements contained all of the features shown, especially in the highly three-dimensional convective region. Nonetheless, the depicted structure is consistent with material presented in Sections 5 and 6, and with the results of OL.

A prominent aspect of the squall system's circulation (summarized in Fig. 10) is that a horizontal influx of air occurred through a deep layer at the front of the storm and continued rearward, dominating the internal circulation. Rear-to-front relative flow (stippled in Fig. 10) was found only 1) in the upper reaches of the leading anvil, 2) in the low-level downdraft outflow and 3) at the extreme rear of the echo in association with the notch. The prevailing rearward relative motion was maximized in a layer just above the melting level. An explanation for this maximum front-to-rear current at midlevels remains elusive. Acceleration of air parcels into a mesolow

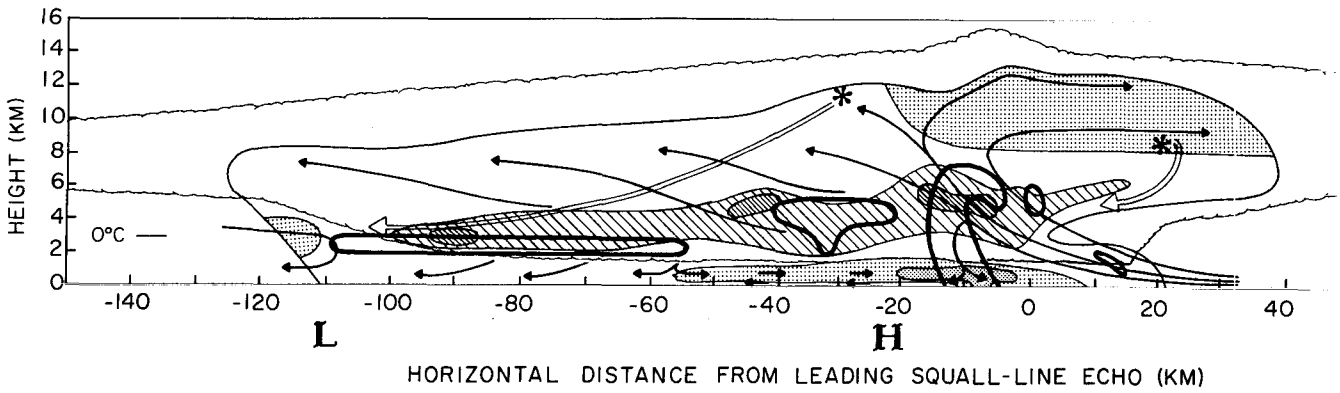

FIG. 10. Conceptual model of 22 May 1976 squall-line system viewed in cross section at maturity. Prominent features of system structure are displayed schematically in a plane transverse to the leading convective line and extending rearward through the portion of the trailing stratiform region occupied by the notch. The abscissa marks horizontal east–west distance (X), which is perpendicular to the convective line, parallel to the system's motion, and measured from the leading echo edge shown on 0.8° elevation scans by the NSSL WSR-57 radar [consistent with coordinate system defined by Ogura and Liou (1980)]. The ordinate denotes height above ground level (Z). System motion is from left to right at 15 m s^{-1}. Outermost scalloped line shows extent of cloud deduced from rawinsonde data and satellite measurements of cloud-top temperature. Contour solid contour marks boundary of detectable radar echo in which reliable Doppler velocity measurements could be made, while heavy solid lines enclose more intense reflectivity features described in text. Stippling indicates regions of system-relative horizontal wind directed from left to right with darker stippling representing stronger flow. Elsewhere within the echo, relative flow is directed from right to left (front to rear). A jet maximum of this flow at midlevels is shown by hatching, with embedded velocity maxima denoted by finer, darker hatching. Thin streamlines show two-dimensional relative flow consistent with Doppler horizontal velocities, echo structure, individual rawinsonde observations, and are appropriate the vertical velocity analysis of Ogura and Liou (1980). Hypothesized ice particle trajectories are depicted by asterisks and trailing arrows. "H" and "L" locate mesohigh and wake mesolow features observed in surface pressure traces. The 0°C level is shown at the rear of the echo.

associated with the cyclonic vortex in the trailing stratiform region might be involved. Acceleration into a midlevel mesolow was detected by Sanders and Emanuel (1977) in their case study of an Oklahoma convective system, and a strong mesolow in the midtroposphere of the stratiform region was found by Brown (1979) in his numerical simulation of a tropical squall system (see his Fig. 13). However, prominent convective-scale velocity maxima superimposed on the rearward current in the leading convective region (evident in many of the cross sections examined) suggest that in our case convective cell dynamics may also have, in some way, contributed to or driven the current. Whatever its explanation, the pervasive front-to-rear relative flow promoted the broad structure of the squall system by transferring ice particles out of the convective region into the stratiform region. As these particles fell, they melted and produced the 50–100 km wide bright band characterizing the stratiform region on radar. The midlevel rearward current eventually met the rear inflow associated with the notch. The sloping interface between these two opposing flows effectively marked the base of the trailing stratiform cloud (shown by a scalloped boundary in Fig. 10).

The data presented here have focused on the description of the 22 May 1976 system's life cycle and its internal precipitation and kinematic structure viewed in cross sections transverse to the system's leading convective line. Future installments of this work are anticipated to describe results of the dual-Doppler analysis and a detailed examination of NSSL soundings for this case. The former will allow a description of airflow and reflectivity variations in the along-line direction, while the latter will extend the kinematic analysis beyond the bounds of the radar echo and augment this extended analysis with thermodynamic data essential to its proper interpretation. Careful examination of sounding data may also elucidate further the apparent relationship of the midlevel rear inflow and notch to the forward acceleration of the leading convective line.

Acknowledgments. The encouragement and support of Dr. Edwin Kessler, Director of NSSL, are appreciated. Dr. Peter S. Ray, Mr. Donald W. Burgess and Mr. William C. Bumgarner of NSSL and Dr. John McCarthy of the National Center for Atmospheric Research provided the authors with valuable information and advice about the data used in this study. Ms. Kay Moore drafted many of the figures. This work was supported by NSSL under Grant NA80RAD00025, and by the National Science Foundation under Grant ATM80-17327.

REFERENCES

Atlas, D. Hardy, K. R., Wexler, R. and R. J. Boucher, 1963: On the origin of hurricane spiral rainbands. *Geofis. Int.*, **3**, 123–132.

Battan, L. J., 1973: *Radar Observation of the Atmosphere*, University of Chicago Press, 324 pp.

Brown, J. M., 1979: Mesoscale unsaturated downdrafts driven by rainfall evaporation: A numerical study. *J. Atmos. Sci.*, **36**, 313–338.

Browning, K. A., J. C. Fankhauser, J. P. Chalon, P. J. Eccles, R. C. Strauch, F. H. Merrem, D. J. Musil, E. L. May and W. R. Sand, 1976: Structure of an evolving hailstorm. Part V: Synthesis and implications for hail growth and hail suppression. *Mon. Wea. Rev.*, **104,** 603–610.

Carbone, R. E., 1982: A severe frontal rainband. Part I: Stormwide hydrodynamic structure. *J. Atmos. Sci.*, **39,** 258–279.

Churchill, D. D., and R. A. Houze, Jr., 1984: Development and structure of winter monsoon cloud clusters on 10 December 1978. *J. Atmos. Sci.*, **41,** 933–960.

Fankhauser, J. C., 1971: Thunderstorm–environment interactions determined from aircraft and radar observations. *Mon. Wea. Rev.*, **99,** 171–192.

Fritsch, J. M., and R. A. Maddox, 1981: Convectively driven mesoscale weather systems aloft. Part I: Observations. *J. Appl. Meteor.*, **20,** 9–19.

Fujita, T. T., 1955: Results of detailed synoptic studies of squall lines. *Tellus*, **7,** 405–436.

——, 1981: Tornadoes and downbursts in the context of generalized planetary scales. *J. Atmos. Sci.*, **38,** 1511–1534.

Gamache, J. F., and R. A. Houze, Jr., 1982: Mesoscale air motions associated with a tropical squall line. *Mon. Wea. Rev.*, **110,** 118–135.

Houze, R. A., Jr., 1977: Structure and dynamics of a tropical squall-line system. *Mon. Wea. Rev.*, **105,** 1540–1567.

——, 1981: Structures of atmospheric precipitation systems: A global survey. *Radio Sci.*, **16,** 671–689.

——, and A. K. Betts, 1981: Convection in GATE. *Rev. Geophys. Space Phys.*, **19,** 541–576.

——, and P. V. Hobbs, 1982: Organization and structure of precipitating cloud systems. *Advances in Geophysics*, Vol. 24, Academic Press, 225–315.

——, and E. N. Rappaport, 1984: Air motions and precipitation structure of an early summer squall line over the eastern tropical Atlantic. *J. Atmos. Sci.*, **41,** 553–574.

Leary, C. A., 1984: Precipitation structure of the cloud clusters in a tropical easterly wave. *Mon. Wea. Rev.*, **112,** 313–325.

——, and R. A. Houze, Jr., 1979a: The structure and evolution of convection in a tropical cloud cluster. *J. Atmos. Sci.*, **36,** 437–457.

——, and ——, 1979b: Melting and evaporation of hydrometeors in precipitation from anvil clouds of deep tropical convection. *J. Atmos. Sci.*, **36,** 669–679.

——, and E. N. Rappaport, 1983: Internal structure of a mesoscale convective complex. *Preprints, 21st Conf. Radar Meteorology,* Edmonton, Amer. Meteor. Soc., 70–77.

Maddox, R. A., 1980: Mesoscale convective complexes. *Bull. Amer. Meteor. Soc.*, **61,** 1374–1387.

——, 1983: Large-scale meteorological conditions associated with midlatitude, mesoscale convective complexes. *Mon. Wea. Rev.*, **111,** 1475–1493.

Newton, C. W., 1950: Structure and mechanisms of the prefrontal squall line. *J. Meteor.*, **7,** 210–222.

——, and J. C. Fankhauser, 1964: On the movements of convective storms, with emphasis on size discrimination in relation to water budget requirements. *J. Appl. Meteor.*, **3,** 651–668.

Ogura, Y., and M. T. Liou, 1980: The structure of a midlatitude squall line: A case study. *J. Atmos. Sci.*, **37,** 553–567.

Pedgley, D. E., 1962: A meso-synoptic analysis of the thunderstorms on 28 August 1958. *Brit. Meteor. Off., Geophys. Mem.*, No. 106, 74 pp.

Rockwood, A. A., D. L. Bartels and R. A. Maddox, 1984: Precipitation characteristics of a dual mesoscale convective complex. NOAA Tech. Mem. ERL ESG-6. NOAA Environmental Research Laboratories, Boulder, CO, 80302, 50 pp.

Rutledge, S. A., and P. V. Hobbs, 1983: The mesoscale and microscale structure and organization of clouds and precipitation in midlatitude cyclones. VIII: A model for the "seeder-feeder" process in warm-frontal rainbands. *J. Atmos. Sci.*, **40,** 1185–1206.

Sanders, F., and K. A. Emanuel, 1977: The momentum budget and temporal evolution of a mesoscale convective system. *J. Atmos. Sci.*, **34,** 322–330.

Zipser, E. J., 1969: The role of organized unsaturated convective downdrafts in the structure and rapid decay of an equatorial disturbance. *J. Appl. Meteor.*, **8,** 799–814.

——, 1977: Mesoscale and convective-scale downdrafts as distinct components of squall-line circulation. *Mon. Wea. Rev.*, **105,** 1568–1589.